COMPARISON OF IBC WITH ACTIVE CONTROLLERS USING A CONVENTIONAL SWASHPLATE TO SUPPRESS GROUND AND AIR RESONANCE

G. Tettenborn, Ch. Kessler, G. Reichert

Institute of Flight Mechanics and Space Flight Technology
Technical University of Braunschweig, Germany

Abstract

Hingeless and bearingless rotor designs are today well accepted for modern helicopters. Compared to articulated rotors, hingeless and bearingless rotors show several advantages like improved flying qualities, reduced maintenance efforts and higher reliability. Continued development, however, revealed some deficiencies in the area of aeromechanical stability and vibration.
In general there is a good basic understanding how to avoid these instabilities. But since it becomes more and more desirable to focus rotor design on aerodynamic features and flight performance, aeromechanical instabilities gain new importance due to the difficulties of providing the required damping. These aeromechanical instabilities are known as ground and air resonance.
Since all rotor concepts suffer from the lack of sufficient natural lead-lag or in-plane damping, most current designs use artificial lead-lag damper. On the other hand, active control offers the possibility for an artificial stabilization of aeromechanical instabilities, becoming a major research activity nowadays.
The paper shortly repeats the problem of aeromechanical instabilities of hingeless rotor-systems. A simple model of a hingeless rotor helicopter including flap, lag, and pitch as the rotor's DOF's, six rigid body DOF's and a dynamic inflow model is used to derive the coupled set of differential equations. An ordering scheme is applied to reduce the complexity of the system equations. The main emphasis of this paper is to demonstrate the potential of active control and to gain physical understanding. A controller using body or rotor multiblade states is compared to an Individual Blade Controller. The feedback gains of the two control concepts are being optimized for both ground and air resonance in hover. Moreover, for the Individual Blade Controller the gains are being computed for an isolated rotor blade and the coupled rotor body system. Both sets of feedback gains are compared to each other in respect of ground and air resonance in hover and forward flight.

Notations and Abbreviations

a	blade hinge offset
$c = 2b$	blade chord
$C_{a\alpha}$	blade lift curve slope
C_{d0}	blade profile drag coefficient
C_{m0}	blade profile moment coefficient
d	structural damping of blade and body
D	damping ratio
f	fuselage parasite drag area
G_{xi}	feedback gain for state variable x_i
h	offset of rotor hub from c.g.
I	body moment of inertia
I_{Bl}	flap and lag moment of inertia about hinge
I_θ	torsional moment of inertia about blade c.g.
m_{Bl}, m_F	blade and fuselage mass
M_{Bl}	static blade moment of inertia
p, q, r	body rates
$\underline{\underline{Q}}$	state vector weighting matrix
R	rotor radius
$\underline{\underline{R}}$	weighting matrix of control inputs
$\underline{\mathbf{u}}$	vector of control inputs
$\underline{\mathbf{x}}$	state vector
y_C	blade c.g. offset from elastic axis
y_L	blade a.c. offset from elastic axis
x, y, z	body translational coordinates
β	flap angle
γ	blade lock number
Δ	perturbation
ε	small parameter
ζ	lead–lag angle
ϑ	control input
θ	blade torsional angle
λ_i	induced inflow
μ	advance ratio
ϕ	feedback phase (SAS–system)
σ	real part of an eigen value
Φ, Θ, Ψ	EULER angles
ψ	blade azimuth angle
Ω	rotor rotational speed
ω	eigen frequency
0, d	collective, differential
C, S	cyclic sine and cosine
nom	nominal
$(\dot{\ })$	$\partial(\ )/\partial t$

1 Introduction

Since the 1960's there has been considerable interest in hingeless rotors because of greater reliability through mechanical simplification, reduced drag, weight and maintenance costs and better handling qualities and maneuverability through increased control power [1].

To achieve further design simplicity, in recent years even bearingless rotors have been successfully developed and applied to many helicopters (EC135, MD Explorer, Bell 430). Important parameters in designing hingeless/bearingless rotors are blade flapping and lagging frequencies [2, 3]. A flap frequency of 1.10-1.15/rev was typical for the first successful hingeless rotors. The current trend is to require lower flap frequencies of about 1.06-1.08/rev, favourable for reduced vibration and gust response and minimizing adverse handling qualities effects at high speed. Regarding the lead-lag frequency, the rotor system can be devided in two destinct groups : soft-inplane rotors with $\omega_\zeta/\Omega < 1$ and stiff-inplane rotors $\omega_\zeta/\Omega > 1$. To achieve manageable inplane bending stresses and vibrations, hingeless rotors are usually designed as soft-inplane rotors with a frequency above 0.6/rev and below 0.8/rev. However, soft-inplane rotors may be susceptible to certain rotor-body aeromechanical instabilities, commonly denoted as ground resonance when the helicopter is on the ground and air resonance when the helicopter is in flight [4, 5, 6]. Ground resonance is caused by coupling of the low frequency regressing lead-lag mode with body modes, mainly determined by landing gear charactersitics. Air resonance may occur, if the low frequency regressing lead-lag mode couples with airframe pitch or roll mode. In contrast to the soft-inplane rotor, stiff-inplane rotors are in general free from ground resonance, but may show flap-lag-torsion instability of the isolated blade [7, 8, 9].
To prevent these instabilities, sufficient lead-lag damping has to be provided. This can be done by simply adding mechanical dampers, leading to higher operational costs, or by increasing structural damping, which on the other hand could require sophisticated material concepts [10]. Additional damping can be produced by relying on aeroelastic couplings. The principal couplings of interest are negative pitch-lag coupling and flap-lag structural coupling [1, 11, 12, 8, 13]. But aeroelastic designs must also consider variations of configuration or operating conditions that may have an adverse effect on the aeromechanical stability. Finally, Active Control Technology (ACT) seems to be an effective approach for artificially increasing lead-lag damping and thus enabling the rotor design process to primarily focus on blade loads. Using automatic control inputs based on vehicle body motion and/or rotor state feedback has become highly feasible, since future rotorcraft will find available ever more capable electronic and computerized control systems. Full authority Fly-by-Wire (or even Fly-by-Light) systems can be designed with advanced control laws, being able to adapt the helicopter's response to the pilot's control objectives and thus reducing the pilot's workload [14]. Until now the safety of flight issues associated with automatic stabilization of unstable or weakly damped modes is still critical and requires highly redundant control systems and quality assurance. But due to rapid advancements in these systems, the application of ACT concepts to suppress ground and air resonance in future rotorcrafts becomes very likely.

Several authors examined the possiblities of suppressing ground and air resonance by ACT using a conventional swashplate [15, 16, 17, 18, 19, 20]. Early work was done by YOUNG et al. [15]. Feedback of roll attitude and roll rate was effective in suppressing a ground and air resonance instability. Two fundamental studies concerning augmentation of ground resonance were performed by STRAUB and WARMBRODT. The first extends the result of [15] by analysing various body and rotor state feedback systems and the influence of control feedback gain and phase on the instability [16]. In the second paper linear optimal control theory for an articulated rotor helicopter was applied. The gains were obtained from the solving RICATTI's equation. Choosing appropriate feedback signals from this full state compensators, resulted in sufficient lead-lag damping of the closed loop system throughout the considered rotor speed range [17].
TAKAHASHI and FRIEDMANN [18, 19] studied active control of air resonance in hover and in forward flight. A comparison of full state feedback and partial state feedback was made. It was found out that partial feedback of body states does not seem to be a reasonable approach to control air resonance of hingeless rotors. An additional study to augment ground resonance instability was performed by KESSLER [20]. Different controllers using multi-variable feedback of rotor and body states were designed for stabilization of ground resonance at two critical rotor speeds. Applying these controllers to the helicopter in hover led to a dramatic destabilization. Considering a nonlinear landing gear, the transient behaviour from ground to air at high thrust levels could be analyzed. Again, the system became dramatically unstable by using the controllers optimized for the linear system.

To alleviate the conventional helicopter's performance, vibrations and noise limitations, new control technologies are presently at various stages of development, commonly denoted as Higher Harmonic Control (HHC) [21, 22, 23]. HHC offers the possibility of modifying the higher harmonic content of the blade's lift distribution and can be implemented in two ways :

- Through the conventional swashplate actuators (SPC) by adding sinusoidal inputs to the collective and cyclic flight control inputs.
- Directly in the rotating system through individual blade actuators (IBC). Since there is no transformation of control inputs in the rotating system, only IBC will allow control of all harmonics.

IBC can be easily extended to augment blade stability problems by sensing individual blade states in the rotating system. Important work was done by N.D. HAM and R.M. MCKILLIP [24, 25, 26, 27, 28, 29]. The applications of IBC were investigated analytically as well as experimentally [30, 31]. The companies EUROCOPTER DEUTSCHLAND and ZF-LUFTFAHRTTECHNIK are working on an incorporation of IBC in helicopters. Flight and wind tunnel testing at NASA-Ames Research Center was done with a Bo 105 helicopter [32, 33]. The different purposes of IBC are:

- gust alleviation,
- blade stall suppression,
- vibration and noise reduction,
- blade bending stress limitations,
- flapping stabilization at high advance ratios <u>and</u>
- lead-lag damping augmentation.

REICHERT and ARNOLD [34] picked up the idea of controlling ground resonance through a conventional swashplate and compared these results with an IBC approach. The four bladed hingeless rotor was modelled similar to [16]. The first approach was realised by body pitch feedback and resulted in a stabilization of the critical mode. Regarding the isolated lead-lad mode, the IBC concept could easily increase damping but, by considering the coupled rotor-body system, results for suppression of ground resonance were rather poor.
In a next step KESSLER [35] discussed the use of IBC to augment rotor lead-lag damping in hover and forward flight. Feedback of lead-lag rate and deflection were useful to highly damp the lead-lag motion.

Since the results for the isolated blade are very promising, the aim of this paper is to further investigate the potential of IBC concepts for stabilization of ground and air resonance in hover and forward flight. Therefore, in comparison to [34], a more sophisticated coupled rotor-body system is considered. For both cases, ground and air resonance, the results are compared to controllers using the conventional swashplate. Thus, a case oriented evaluation of different control concepts is possible.

2 Mathematical Model

The spatial helicopter model and the 3DOF flap-lag-torsion model of the hingeless rotor blade can be seen in Fig. 1. The blade is assumed rigid rotating against linear springs and dampers about a common hinge, located a distance a out of the rotor axis. This assumption simplifies the equations of motion, while retaining the essential features of ground and air resonance [36]. The hinge sequence is lead-lag inboard, flap and torsion outboard.The flap deflection β is positive up, lead-lag ζ positive forward (in direction of rotation) and torsion θ is positive nose up. Structural flap-lag coupling and precone are modeled but set to zero in this study. Linear twist of the blade is neglected. The rotor hub is located directly above the fuselage c.g..

The fuselage is represented as rigid body with six degrees of freedom, three linear translations and three angular positions, roll, pitch and yaw. The aerodynamic forces on the fuselage are represented by an equivalent flat plate drag. Horizontal or vertical stabilizers are not included. For ground resonance analysis a linear modeled landing gear is included. It consists of three linear springs and dampers for the rotational body modes and three linear springs and dampers for the translational body modes.
The aerodynamic loads of the rotor blades are based on a quasi-steady approximation of GREENBERG's unsteady theory for low reduced frequencies. Thus, the lift deficiency function is taken to be unity. Unsteady aerodynamic effects are accounted for by using a dynamic inflow model, suitable for representing the low frequency unsteady aerodynamics in ground and air resonance analysis [19, 37, 38]. This simple model assumes that the inflow perturbations would respond with a first-order time lag to perturbations in the rotor loads. In the present paper, the model of PITT and PETERS [39] is used. Compressibility, dynamic stall effects and reverse flow are neglected.
The differential equations are being derived by applying D' ALEMBERT's principle. The equations of motion of the coupled rotor-body system are very large and contain nonlinear terms. To simplify the final set of equations and to retain only the important terms, an ordering scheme is used [19, 36]. The ordering scheme is based on the assumption that

$$O(1) + O(\varepsilon^2) \approx O(1)\ , \qquad (1)$$

which states that terms of order ε^2 are negligible compared to terms of order unity. The quantity ε is a non-dimensional parameter, which quantifies the meaning of a small parameter. A quantity is meant to be small, if it reaches values between $0.1 < \varepsilon < 0.2$.
The symbolic manipulation programm REDUCE is used to generate the nonlinear equations of the rotor-body system, consisting of six fuselage equations and three rotor blade equations for each blade. In addition, the aerodynamic thrust, roll and pitch moments at the hub center are determined for the perturbation aerodynamics in the dynamic inflow model. For stability analysis, the set of equations is linearized about a blade equilibrium solution and a helicopter trim solution, extracted simultaneously by using harmonic balance. Propulsive trim determines the free flight equilibrium solution and requires the calculation of pilot settings $\vartheta_0, \vartheta_C, \vartheta_S$, as well as the vehicle motion and orientation. This study is restricted to level flight. Moment trim is used for prescribed pilot settings and vehicle orientation, offering the possibility to analyse the system stability under more academic conditions. After linearization, a multiblade transformation is applied, which transforms the set of rotating blade degrees of freedom to a set of hub fixed non-rotating coordinates [40, 41]. For a four bladed helicopter with

flap-lag-torsion rotor blade model, this is done by

$$\beta_k = \beta_0 + \beta_C cos\psi_k + \beta_S sin\psi_k + \beta_d(-1)^k, \quad (2)$$
$$\zeta_k = \zeta_0 + \zeta_C cos\psi_k + \zeta_S sin\psi_k + \zeta_d(-1)^k, \quad (3)$$
$$\theta_k = \theta_0 + \theta_C cos\psi_k + \theta_S sin\psi_k + \theta_d(-1)^k . \quad (4)$$

This transformation is particularly advantageous in analysing stability of coupled rotor-body systems. In hover, the transformed system has constant coefficients (assuming all blades identical) and it decouples the set of equations in a collective, a differential and cyclic part. It reduces the periodicity in the equations, making constant coefficient analysis possible at low advance ratios. Besides, it provides a better physical interpretation of the results than individual blade degrees. Finally, an active control device has to be incorporated in the mathematical model. The pitch of the k-th rotor blade is given by

$$\vartheta_k = (\vartheta_0 + \Delta\vartheta_0) + (\vartheta_C + \Delta\vartheta_C)\, cos\psi_k + (\vartheta_S + \Delta\vartheta_S)\, sin\psi_k + \Delta\vartheta_d . \quad (5)$$

The terms with Δ are small and represent the active control inputs, while the others are the pilot settings. Note, that through implementation of an differential contol input $\Delta\vartheta_d$, individual blade control can thus be achieved in the non-rotating system [25].
After a state space transformation, the system is rewritten in first order form and consists of 39 states, inclusive of the three states for the dynamic inflow model $\lambda_{i0}, \lambda_{iC}, \lambda_{iS}$ (the perturbation symbol Δ for the states and the controls is neglected) :

$$\dot{\underline{x}} = \underline{\underline{A}}(\psi)\underline{x} + \underline{\underline{B}}(\psi)\underline{u}, \quad (6)$$

with the states $\underline{x} = [\theta_0, \theta_C, \theta_S, \theta_d, \beta_0, \beta_C, \beta_S, \beta_d, \zeta_0, \zeta_C, \zeta_S, \zeta_d, x, y, z, \Phi, \Theta, \Psi, \lambda_{i0}, \lambda_{iC}, \lambda_{iS}, \dot\theta_0, \dot\theta_C, \dot\theta_S, \dot\theta_d, \dot\beta_0, \dot\beta_C, \dot\beta_S, \dot\beta_d, \dot\zeta_0, \dot\zeta_C, \dot\zeta_S, \dot\zeta_d, \dot x, \dot y, \dot z, p, q, r]^T$ and four control inputs $\underline{u} = [\vartheta_0, \vartheta_C, \vartheta_S, \vartheta_d]^T$. $\underline{\underline{A}}(\psi)$ is the 2π-periodic system matrix and $\underline{\underline{B}}(\psi)$ is the 2π-periodic control matrix.
Stability can now be determined by using either an eigenvalue analysis or FLOQUET theory for the periodic problem in forward flight [41]. The FLOQUET transition matrix is computed numerically, using a fourth order RUNGE-KUTTA procedure. The eigen values of the transition matrix are the characteristic multipliers. With these characteristic multipliers, the characteristic exponents $\lambda = \sigma + j\,\omega,\ j = \sqrt{-1}$ can be calculated except an integer multiple of 1 in the imaginary part. In hover, the system matrices show constant coefficients and the eigen values can be computed directly from the system matrix $\underline{\underline{A}}$. Since the imaginary part must change smoothly by increasing μ the right eigen frequency can be figured out from the hover value. The system is stable, if for all eigen values $\sigma < 0$ holds.

Rotor Data			
$\bar{R}$	4.9m	$\bar{\Omega}$	44.5/s
N_{Bl}	4	$C_{a\alpha}$	5.9
I_{Bl}	0.19	C_{d0}	0.01
M_{Bl}	0.36	C_{m0}	-0.02
$\bar{m}_{Bl}$	23.4kg	γ	5.0
I_θ	0.0001	ω_β	1.12
a	0.15	ω_ζ	0.67
c	0.055	ω_θ	3.2
y_C	0.0	y_L	0.0
d_β	0.0	d_ζ	0.5%
d_θ	0.0		

Fuselage Data			
h	0.3	$\bar{m}_F$	1906.4kg
f	0.8	I_{xx}	2.5
I_{yy}	8.5	I_{zz}	7.3
I_{xz}	1.2	ω_x	29/s
ω_y	46/s	ω_z	27/s
ω_Φ	19.16/s	ω_Θ	11.68/s
ω_Ψ	23/s	d_x	3%
d_y	3%	d_z	3%
d_Φ	3%	d_Θ	3%
d_Ψ	3%		

Table 1: Data of Nominal Configuration

3 Stability Results

The data used in this study correspond to a four bladed soft-inplane helicopter somewhat similar to the MBB Bo 105. REICHERT and ARNOLD [34] analyzed a similar helicopter, but did not consider the torsional flexibility of the rotor blade and the effects of dynamic inflow, which are meant to be important for ground and air resonance [19, 37]. Furthermore, a conventional landing gear was modeled, resulting in a higher stiffness and therefore in higher body frequencies. As a consequence, the lead-lag regressing mode coalesces with body pitch or roll mode far beyond the nominal rotor speed. In this paper the more interesting case of a helicopter Bo 105 with high landing gear is used, see [20]. Thus, the rotor has to pass the critical rotor speed, being speeded up to nominal rotor speed. The data of the nominal configuration are listed in Tab. 1. Non-dimensionless parameters can be distinguished from dimensionless by the bar (¯).
The low body frequencies result in a coalescence of regressing lead-lag with the body pitch mode at

$\Omega = 93\%\ \Omega_{nom}$ and with the body roll mode at $\Omega = 109\%\ \Omega_{nom}$. In Fig. 2 the real part of the isolated blade lead-lag motion and regressing lead-lag of the coupled rotor-body system is plotted versus the lead-lag structural damping d_ζ for medium thrust and full thrust at $\Omega = 93\%\ \Omega_{nom}$. As can be seen the chosen value $d_{\zeta,nom} = 0.5\%$ is not sufficient to avoid a ground resonance instability, whereas the isolated blade will not have stability problems. If the helicopter is in hover, air resonance instability is only possible for values $d_\zeta < 0.15\%$. Therefore, regressing lead-lag of the nominal configuration will be slightly damped in hover. Although, increasing thrust will increase damping of the isolated blade, damping of the coupled rotor-body system will decrease, especially for the helicopter on ground [42].

In Fig. 3 an eigen value calculation for the helicopter on ground was performed in a rotor speed range from 0% to 120% at zero thrust. The eigen modes were identified at nominal rotor speed. The 39 states result in 19 complex conjugated values and one real eigen value for the collective part of the dynamic inflow. The typical curve for the lead-lag regressing mode can be clearly identified. The curve for the progressing lead-lag mode is not fully visible. The collective lead-lag mode couples with body yawing mode. The curve for the differential lead-lag mode is very similar to the collective lead-lag, but of lower frequency. Furthermore, the figure shows highly coupled low frequency eigen modes for regressing flap and dynamic inflow [43]. Because of the influence of centrifugal forces, the remaining flapping modes $\beta_0, \beta_{prog}, \beta_d$ rise faster with varying rotor speed, compared to the lead-lag modes. Due to the higher frequencies, the torsional rotor modes are not visible. The body longitudinal and lateral translations couple with lead-lag cyclic modes, whereas the body vertical translation couples with collective flap. Another coupling of rotor and body modes exits between body roll and pitch mode with cyclic flap. The relatively low eigen frequencies of the body pitch Θ/β_C and roll mode Φ/β_S leads to a coalescence of the regressing lead-lag mode at 93% and 109% Ω_{nom}, respectively. Another coalescence occurs beyond 120% Ω_{nom}, but will not be discussed, in detail. At the above mentioned rotor speeds, the coupling between regressing lead-lag and body rotational modes results in an instability characterizing the ground resonance case. Consequently, the weaker damped eigen mode will be destabilized and the better damped eigen mode will be stabilized. This is illustrated in the figure by the opposite peaks for the real parts at resonance rotor speed. Similar results are presented in [20, 44]. Although, for hingeless rotor blades the body pitch and roll mode are coupled with flapping, the landing gear stiffness characteristics dominate these body frequencies. On the other hand, aerodynamic forces provide effective rotor-body damping somewhat analogous to landing gear dampers [10].

In Fig. 4 an eigen analysis was performed for the helicopter in hover for moment trim at $\vartheta_0 = 0°$. Since in case of moment trim thrust must not compensate helicopter weight, rotor speed could be varied again from 0% to 120%. The curves for rotor flap and lead-lag eigen frequencies resemble the curves in Fig. 3, except rotor flap regressing mode. This is typical for the airborne state, since loosing ground contact the influence of the landing gear vanishes. Thus, the body roll and pitch modes are determined by a strong coupling with regressing flap mode. The regressing flap mode cannot be clearly identified, but two oscillatory body pitch and roll modes with high content of regressing flap arise. These coupled eigen frequencies are mainly determined by the blade flap stiffness and body inertias [42, 45, 46]. In addition, the high damping of the cyclic flapping mode enters into the system dynamics, acting in some respect like body damping [2]. Above the cross-over rotational speed at $\Omega = 26.5/s$, there exist two rotor speed ranges where a coalescence between regressing lead-lag and body modes leads to a destabilization. Lead-lag regressing couples with body pitch Θ/β_C at about 70% Ω_{nom} and with body roll Φ/β_S at 92% Ω_{nom}. The last case is of higher interest, if realistic operating conditions in flight are investigated. Both couplings are not as severe as for the helicopter on ground. This could be an effect of the lower body frequencies in air, which typically tends to weaken aeromechanical instability. In addition, body roll mode Φ/β_S at 92% Ω_{nom} shows higher damping levels compared to the body pitch mode on ground. This again leads to a less intensive coupling for the helicopter in air.

Fig. 5 shows the weakly damped eigen modes of the helicopter in hover for a rotor speed range from 80% to 120% Ω_{nom}, using propulsive trim. This rotor speed range seems to be more realistic, if rotor speed optimization in future rotorcrafts will become available [14]. The modes are denoted by using conventional flight mechanics notations. As already been discussed in Fig. 1, the real part of lead-lag regressing at frequency coalescence with body roll mode for 92% Ω_{nom} is still negative and therefore the helicopter is free from air resonance. The critical damping value of regressing lead-lag for this configuration in hover is $D_\zeta = 0.8\%$. Phugoid and Dutch Roll are almost of same frequency, whereas Spiral and Vertical are aperiodic motions. A weak instability exists for the Phugoid, typical for a helicopter in hover [41, 47]. The Dutch Roll is slightly stable and the Spiral is less damped than the vertical motion.

To analyze the behaviour in forward flight, Fig. 6 shows the real part of the lead-lag motion for the isolated blade and regressing lead-lag versus the advance ratio. The stability of the isolated blade was determined in the rotating frame. The lead-lag damping of the isolated blade starts at a moderate value in hover and decreases to a minimum value at $\mu \approx 0.22$, before increasing for advance ratios beyond this value. Regarding an isolated blade, a flap-lag-torsion instablity can occur, but usually this is only a problem to stiff-inplane rotors. The present system models a soft-inplane rotor, which is stable within the whole flight regime. The curve's characteristic corresponds to the power required curve of a helicopter. In contrast to the isolated blade, lead-lag regressing damping starts at a value four times smaller and nearly monotonly increases with advance ratio. Consequently, the characteristics of both curves differ extremly for advance ratio below $\mu = 0.3$. Since the body and lead-lag frequencies do not change with increasing advance ratio, this different behaviour of the coupled rotor-body system might be caused by increased body damping. In fact, especially body roll damping also monotonly increases in this range of advance ratios and thus resembles the curve for regressing lead-lag damping. On the other hand, for advance ratios beyond $\mu = 0.3$ regressing lead-lag damping seems to be more dominated by the behaviour of the isolated blade.

The remaining part of this paper deals with the potential of active control to suppress ground and air resonance. For the present configuration, ground resonance is possible for a rotor speed of $\Omega = 93\% \ \Omega_{nom}$. Different active controller will be optimized for this interesting case being within the range of operating conditions on ground. The helicopter in airborne condition does not encounter air resonance instabilities. Therefore, different controllers will be optimized for the case of minimal regressing lead-lag damping at $\Omega = 92\% \ \Omega_{nom}$ in hover and forward flight. The behaviour of the closed loop system with varying rotor speeds will be analyzed.

3 Active Control to Suppress Ground and Air Resonance

In the following paragraph the possibilities and mechanisms of suppressing aeromechnical instabilities are discussed. In order to select promising control structures, the impact of control inputs on the rotor and body eigen modes as well as the links between these two subsystems has to be considered. This will help to gain physical insight in rotor dynamics and to evaluate the effectiveness of different control loops.

Fig. 7 provides a general scheme of rotor body interactions and summerizes feasible concepts to overcome aeromechanical instabilities.

The fundamental objective of any solution is to control the rotor and body eigen modes involved in the instabilitites by changing blade pitch. The first possibility arises, if fuselage states are fed back to the conventional swashplate actuators (SPC). Since the collective control input is merely able to control ground and air resonance, it can be neglected [19]. It is common standard to measure body states such as pitch or roll rate and feed them back to the cyclic control inputs. Implemented in many modern helicopters, such means are designated as Stability Augmentation Systems (SAS). In general their objective is to improve stability and handling qualities. These systems are mostly designed as limited authority low frequency devices in order to prevent interferences with rotor dynamics. According to Straub and Warmbrodt [16], basically two control pathes exist that can influence rotor and body eigen modes through the conventional swashplate :

- The fuselage pitch and roll motion can be controlled through rotor pitch and roll moments arising from flapping. The magnitude of each is directly related to the equivalent blade root hinge offset and blade flapping stiffness.
- Lead-lag damping augmentation through Coriolis coupling with blade flap motion. This requires either steady blade coning or built-in precone.

Thus, feeding back body modes to cyclic control inputs can influence rotor and body dynamics through rotor flapping. On extending the bandwith up to frequencies which is relevant for ground and air resonance, i.e. body roll/pitch or regressing lead-lag, those instabilities can be supressed. The use of SAS for stabilizing aeromechanical instabilities is definitely advantageous, since the whole control system is located in the non-rotating frame and many parts of classical SAS hardware is available. A fundamental study, dealing with such an augmentation system for ground and air resonance, is described in [15]. To further stabilize the system, feedback signals of multiblade rotor states can be used in addition [16, 20]. The system is considerably stabilized but adverse effects, like worsening of handling qualities or destabilizing of other rotor eigen modes have to be accounted for by reducing gains or inclusion of filters into the feedback loop. Finally, if all states of a helicopter are fed back, the results will be the best [17]. This full state feedback is often called Optimal Control (OC). The gains are analytically determined by solving the matrix Riccati equation. The optimal control theory requires the knowledge of all rotor, body and dynamic inflow states, which results in an excessive hardware expense. This is not feasible as a practical solution. To overcome this disadvantage, an observer based controller design may be applied, reducing the amount of sensing. The unmeasured states must be accurately estimated by the observer using a simplified model of the plant. If the model differs seriously from the real, complex system, the closed loop system might encounter severe problems.

As mentioned above, the mechanism of SAS is mainly based on an influence of body modes through rotor flapping. Another way to augment the stability of the lagging motion is to control the individual blade through :

- Coriolis forces
- rotor inplane aerodynamic forces [34].

The latter could not effectively be controlled using cyclic controlls of the conventional swashplate. Several companies are engaged in developing actuators located in the rotating frame to control blade pitch individualy. Primary objective of the R&D efforts is the implementation of Higher Harmonic Control (HHC) to reduce vibration, noise and to improve performance. HHC with actuators in the rotating system has several advantages and does not limit its full potential to Helicopters with 3 or less blades [23, 32]. Of course, HHC is not able to definitely influence system stability, but as soon as such actuators become reliable, the extension to further control tasks will be practicable. The realisation of a ground and air resonance stabilization device would not be a problem of actuator bandwith, as signals up to 6Ω were supplied as pitch input. With the present state of technology the installation of IBC with rotating pitch-actuators attached to the blade's root is not considered to enter overall helicopter service. The system would be too heavy and mechanically complex for the civilian aviation [14]. However, with the emergence of new technologies and materials like *smart materials* and *piezoelectric actuators*, the helicopter industry realizes that this might be the major breakthrough in future rotorcraft design through rotor active control technology. Within the various possibilities of implementing smart materials in the individual rotor blades, the actively controlled servo-flap seems to be a feasible solution [48, 49, 50].

If the HHC hardware will be used for augmenting the stability of the individual blade by feeding back individual blade states, the control system is denoted as Individual Blade Control (IBC) [24, 25, 26, 27, 28, 29]. Note, that IBC not only involves the control of each blade independently, but also a feedback loop for each blade in the rotating system. In these studies the different application of IBC to stabilize the isolated blade or to improve the system's response behaviour are discussed. Ref. [29] particularly deals with the rotor blade lead-lag damping augmentation. For simplification the authors only investigated the concept of controlling lag damping via CORIOLIS forces due to pitch-induced flapping. An individual feedback loop consisting of lag acceleration sensor, integrator, compensator, controller and actuator was related to each blade. Although the blade model in this study was very simple, the concept of IBC proves to be feasible to control lag damping.

Fig. 7 outlines the essential dynamic links between the different subsystems of a helicopter. The flapping, lagging and torsion motion of the isolated blade, which will arise from blade pitch input, generates forces and moments at the rotor hub. Transferred into the non-rotating frame these forces and moments result in collective and cyclic rotor motion. On the other hand, these multiblade eigen modes cause body motions that influence the rotor blade motion, and vice versa. Thus, IBC has an direct impact on the coupled rotor-body system, but primarily controls isolated blade motion.

REICHERT and ARNOLD [34] analyzed the IBC concept for ground resonance suppression. By feeding back lead-lag states, the damping of the isolated blade could be easily increased. However, including the body states for ground resonance calculations, results tended to be unfeasible, compared to a SAS concept. The investigations of the IBC concept were limited to medium thrust condition.

Therefore, KESSLER [35] discussed the use of IBC to augment rotor lead-lag damping in hover and forward flight. Considering the most effective forces and moments of a hingeless rotor blade, the model was more sophisticated than that of [29]. Feedback of lead-lag rate and deflection were useful to highly damp the lead-lag motion without significant manipulation of rotor dynamics and high control effort. Simple controller design for the whole range of advance ratios seems to be possible without scheduling of feedback gains.

Therefore, the idea of controlling ground resonance by means of IBC is picked up again in this paper. But in addition to [34], the investigations are extended to the whole flight regime. The results of the uncontrolled system reveal a less intensive coupling of regressing lead-lag and body modes in airborne condition, which might increase effectiveness of IBC for helicopter in hover and forward flight. Besides, in all former studies the effect of flap feedback signals to pitch input for lead-lag damping augmentation are neglected. It is expected that at least the coupled regressing lead-lag and body eigen modes can be influenced through flapping induced roll and pitch moments, similar to the mechanism of SAS. For evaluation of effectiveness the IBC results are compared to SAS results. To get an idea of the impact of the body modes to the design of feasible IBC controllers, results for the isolated blade will also be considered.

Optimization of the SAS and the IBC controllers for the isolated blade is done by applying optimal output vector theory [51, 52]. The computer program used for determining the gains is described in [53]. A linear quadratic performance index penalizes the entire state vector and control time history. Every state may be penalized although only output variables are fed back :

$$J = \int_0^\infty (\underline{x}^T \underline{\underline{Q}}\, \underline{x} + \underline{u}^T \underline{\underline{R}}\, \underline{u})\, dt\,. \tag{7}$$

The weighting matrices $\underline{\underline{Q}}$ and $\underline{\underline{R}}$ have to be determined favourable for the given control problem.

The IBC controllers for the coupled rotor-body system are optimized using root loci diagrams. Thus, the effect of the different feedback signals on the system can be evaluated. This was found to be important for the present paper, since no comparable studies are available.

The design objective for all controllers is to maximize system stability of the coupled rotor-body system or to augment lead-lag damping of the isolated blade, and to keep the effect on the system's eigen frequencies low. In addition, the control effort has to be limited and balanced for comparable controllers. The control vector is defined as :

$$\underline{u} = -\underline{\underline{G}}\,\underline{y} = -\underline{\underline{G}}\,\underline{\underline{C}}\,\underline{x}\,, \tag{8}$$

where $\underline{\underline{G}}$ is the gain matrix and $\underline{\underline{C}}$ the output matrix. Hence, the closed loop plant matrix becomes

$$\underline{\underline{A}}_{cl} = \underline{\underline{A}} - \underline{\underline{B}}\,\underline{\underline{G}}\,\underline{\underline{C}}. \tag{9}$$

3.1 Helicopter on Ground

Fig. 8 compares open and closed loop eigen values in the complex plane for the helicopter standing on ground. Thrust to weight ratio was set to 50% and rotor speed to 93% Ω_{nom}. Four different controllers - two of each kind - are being compared. The SAS approach uses pure roll and pitch rate for the first controller and in addition cyclic multiblade lead-lag states for the other controller, mentioned to be stabilizing in [16, 54]. The cyclic lead-lag modes can be derived from mast shear-forces or blade bending moment signals [14]. The two Individual Blade Controllers make use of lead-lag states, and lead-lag and flap states, respectively. These signals can be measured directly by the use of tension straps or can be generated from deflection and acceleration signals [31].
The open loop system shows an unstable eigen value in the right part of the complex plane, denoted as lead-lag pitch coupling ζ_{reg}/Θ. This characterizes the ground resonance case, which arises due to the chosen value of structural lead-lag damping $d_\zeta = 0.5\%$. All four controllers stabilize the former unstable eigen mode. The SAS-controllers do not affect most of the eigen values, since the feedback gains remain small. Especially for the simple p-q-controller high gains could be problematic, since progressing lead-lag ζ_{prog} is destabilized [46, 20]. This simple controller slightly stabilizes both, the ζ_{reg}/Θ and the Θ/ζ_{reg} eigen mode. The second SAS-controller results in further regressing lead-lag damping, since more states are being fed back. But unlike the simple SAS-controller, the body mode Θ/ζ_{reg} is slightly destabilized. This shift in damping between the two coupling modes is caused by an artificial decoupling of these eigen modes. Compared to SAS, IBC shows less closed loop damping. Feeding back only lead-lag states $\zeta, \dot{\zeta}$ leads to a stabilization of nearly all modes. This is due to the kinematic coupling of lead-lag and flap mode on the one hand and the coupling of rotor flap and body modes on the other hand. The reached damping level of regressing lead-lag ζ_{reg}/Θ is below the level of the p-q-controller. The eigen frequency of the pitch mode Θ/ζ_{reg} is shifted to lower values. Again, the more states are being fed back, the better the results. However, the second IBC-controller with $\zeta, \dot{\zeta}, \beta, \dot{\beta}$-feedback signal does not reach the damping level of the second SAS-controller. Note, that the lead-lag gains for both IBC-controllers are the same. This time, the flap eigen values are shifted towards higher damping levels without changing the eigen frequencies significantly. This is a direct consequence of the $\dot{\beta}$-feedback signal. Due to the coupling of rotor flap and body modes, the body pitch mode Θ/ζ_{reg} is as well affected by this contoller. But unlike before, the damping of body pitch mode is decreased. This effect is somewhat similar to the influence of the second SAS-controller. Body damping is shifted back between the coupled regressing lead-lag and body pitch mode.
In [34] equivalent results concerning effectiveness of IBC are mentioned. The authors realized that feedback of lead-lag modes can merely stabilize ground resonance. But an interessting new aspect is that feeding back isolated flap states could further contribute to the system's damping level without affecting overall system dynamics.
The SAS concept seems to be favourable for suppressing ground resonance. Even higher damping levels are possible, if the gains of the controller are further increased. The gains and phases of the SAS- and IBC-controllers are presented in Tab. 2, at the end of this paper.

Fig. 9 shows the real part of the open and closed loop system for regressing lead-lag or body modes involved in ground resonance versus rotor rotational speed. Out of these modes only the least stable is plotted. All controllers optimized for $\Omega = 93\%\ \Omega_{nom}$ are unable to suppress ground resonance in the analyzed range of rotor speeds, generally even itensifying instabilities at different coupling points. Scheduling of gains and phases is needed to guarantee stability with varying rotor speed. For the SAS concept controller design with additional feedback loops might be successful in stabilizing the system in the whole range of rotor speeds without scheduling of gains and phases [20]. This seems to be more complicated for IBC-controllers, since the influence of the different feedback loops on the coupled rotor-body modes changes extremly especially in case of flap states for varying rotor speed. Thus, the $\zeta, \dot{\zeta}$-controller results in better damping levels at $\Omega = 109\%\ \Omega_{nom}$. But Fig. 9 also clarifies that this simple IBC-controller only slightly improves system damping, but mainly results in a frequency shift of coalescence points. For rotor speeds where the interaction of body modes and lead-lag regressing is low, damping levels of the IBC-controllers are better than the SAS-controllers, for example around nominal rotational speed $\Omega_{nom} = 44.5/s$.

Fig. 10 presents time history results of the isolated blade and the coupled rotor-body system for open and closed loop. A comparison of the simple $\zeta, \dot{\zeta}$-controller for both systems is made. Lead-lag angle is given in the rotating system. As discussed before, the damping ratio $D_\zeta = 1.2\%$ of the isolated blade at F/mg = 50% without feedback is not sufficient to avoid ground resonance. Closing the feedback loops with the gains optimized for the coupled rotor-body not only stabilizes the coupled rotor-body system, but also increases damping ratio of the isolated blade to 1.78%. The gains optimized for the isolated blade even results in a damping ratio of 5.54%. This value achieved by mechanical lead-lag damper would be sufficient to avoid ground resonance. However, including fuselage motion, the feedback gains determined for the isolated blade reduces damping of the coupled rotor-body system. Comparing the sets of gains for both cases, it can be seen that the sign of G_ζ is opposite, indicating a phase shift of 180° for the lead-lag angle response. This result disproves the idea of optimizing an IBC system for the isolated blade will succeed in suppressing instabilities of the coupled rotor-body system. At least for ground resonance with its strong interaction between body and regressing lead-lag motion this methode is not suitable. In [34] similar results are stated, except for the closed loop damping of the isolated blade with gains chosen for the coupled rotor-body system. Contrary to the present paper, the isolated blade was destabilized, very likely to be caused by the different configuration of the model.

This paragraph outlines that ground resonance can be improved through the use of IBC, but the consideration of an isolated blade is not suitable. Compared to an SAS approach, the results are poor.

3.2 Helicopter in airborne state

Fig. 11 compares open and closed loop eigen values in the complex plane for the helicopter in hover. Propulsive trim at 92% Ω_{nom} has been used. Again, four different controllers with the feedback loops discussed in the previous paragraph are being compared. All controllers stabilize the regressing lead-lag mode, but in opposite to the helicopter standing on ground the SAS-controllers show lower closed loop damping. Starting with a damping ratio of 0.8% in the open loop case, the simple p-q-controller increases the damping ratio to 1.3%, whereas the second SAS-controller improves damping ratio to 3.0%. Compared to ground resonance, the effectiveness of the SAS-controllers is reduced and gains must be higher. On the other hand, body modes are mainly determined by the flapping characteristics. Thus, swashplate pitch inputs caused by SAS feedback loops have an increased impact on the body modes. In combination with the high gains this can result in extremly modified handling qualities of the helicopter. To lower the effect of the SAS-controllers on the body modes, filters have to be implemented in the feedback loops. Especially for the second SAS-controller with cyclic lead-lag states feedback signals controller design without filters definitly seems not to be possible. The filters used for the present paper are not suitable enough to prevent the impact on the eigen frequency of the pitch mode Θ/β_C. Additional filters could also weaken the destabilization of the progressive flap mode. For the helicopter in airborne condition the IBC concept is preferable. Even with the simple $\zeta,\dot{\zeta}$-controller the damping ratio is increased to 8.8%. The effect on the low frequency body eigen modes and roll mode is negligible. Except for the pitch mode, since this simple controller leads to a destabilization and a rise in eigen frequency. This influence is considered as an important constraint for further $\zeta,\dot{\zeta}$-controller designs. The flap eigen modes are also affected by a decrease in damping and eigen frequency. To overcome these disadvantages of the $\zeta,\dot{\zeta}$-controller, additional feedback of flap states can be implemented in the controller design. This second IBC-controller does not affect overall system dynamics and increases damping of nearly all eigen modes. Note that for all IBC-controllers no filter design was considered. The damping ratio of regressing lead-lag is increased to 17.0%, questionable to be possible for both SAS-controllers. The gains and phases of the SAS- and IBC-controllers are presented in Tab. 3.

This investigation clarifies that IBC is very effective for augmenting regressing lead-lag damping in airborne condition. This is due to a less intensive coupling of body and regressing lead-lag mode. Thus, the damping of the lead-lag motion is mainly determined by the isolated blade damping, favourable for the applicability of the IBC concept. Furthermore, the effect on body modes is small. Additional feedback signals of flap states increases damping of all modes, inclusive of regressing lead-lag, and is able to overcome problems with system dynamics.

Fig. 12 shows the real part of the open and closed loop system for regressing lead-lag or coupling body modes versus rotor rotational speed for the helicopter in hover. Out of these modes only the least stable is plotted. The simple p-q-controller could nearly maintain the improved but still low damping level in the whole range of rotor speeds. Contrary, the second SAS-controller even gets less stable compared to the open loop case for rotor speeds above 110% Ω_{nom}. Again gain scheduling or different controller designs might be a solution for this problem. Since the rise in damping is enormous for the IBC-controllers, gain scheduling is not necessary. Although the damping level decreases for both IBC-controllers if rotor speed goes down, the system is still more stable than in open loop case. For rotor speeds above nominal rotational speed $\Omega_{nom} = 44.5/s$ damping only slightly decreases. It is obvious that the $\zeta,\dot{\zeta},\beta,\dot{\beta}$-controller reduces the coupling of body modes and regressing lead-lag at 92% Ω_{nom}, since damping levels of both IBC-controllers are nearly the same for rotor speeds where no frequency coalescence exist. Consequently, feedback of flap states primarily influence body and of course flap eigen modes and only secondly lead-lag motion through kinematic flap-lag coupling.

In Fig. 13 open and closed loop regressing lead-lag damping is plotted versus the advance ratio μ at 92% Ω_{nom}, applying the gains optimized for hover. The closed loop system with the simple p-q-controller is less damped than the open loop system beyond advance ratios of 0.2. The second SAS-controller stabilizes the system for all advance ratios. Starting with its hover value, damping decreases first to a local minimum at $\mu = 0.1$, then the curve resembles the curve for the open loop case. Both IBC-controllers provide high damping levels throughout the whole flight regime. Of course, the enormous damping margin for the design point cannot be maintained in forward flight, although the decrease in damping for medium advance ratios is less intense for the simple $\zeta, \dot{\zeta}$-controller. The local minimum for the $\zeta, \dot{\zeta}$-controller is found at $\mu = 1.8$ and for the $\zeta, \dot{\zeta}, \beta, \dot{\beta}$-controller at $\mu = 2.6$. The rise in damping for advance ratio beyond the local minimum is stronger than for the SAS-controller. Thus, the regressing lead-lag damping curves of the IBC systems look somehow similar to those of the isolated blade.

Since the results for the IBC concept are very promising, further investigation has been done for this approach.

In Fig. 14 closed loop damping for the lead-lag motion of the isolated blade and regressing lead-lag is plotted versus advance ratio at 92% Ω_{nom}. Lead-lag damping of the isolated blade has been obtained by optimizing two controllers - one for $\zeta, \dot{\zeta}$- and the second for $\zeta, \dot{\zeta}, \beta, \dot{\beta}$-feedback - for the isolated blade. Again, the design point for the controllers is the hovering helicopter. Thus, both closed loop systems - isolated blade and coupled rotor-body system - can be directly compared. The gains for both systems are presented in Tab. 4, at the end of this paper. In hover, the closed loop sytems of the isolated blade are better damped than the coupled rotor-body system with $\zeta, \dot{\zeta}, \beta, \dot{\beta}$-controller. However, the decrease in damping for medium advance ratios is more intense for the isolated blade. Thus, the curves of regressing lead-lag damping get closer to the curves of lead-lag damping increasing the advance ratio. Comparing the gains of the IBC-controllers for both systems, it is obvious that regressing lead-lag dynamics are mainly dominated by the characteristics of the isolated blade, at least for the hover design point. Contrary to ground resonance, all gains show the same sign and furthermore approximately the same value for deflection feedback. These results recall the idea to optimize an IBC-controller for an isolated blade and applying the gains to the coupled rotor-body system.

This has been done in Fig. 15, which shows regressing lead-lag damping versus advance ratio at 92% Ω_{nom}. The IBC-gains have been optimized for the isolated blade in hover. Both IBC-controllers result almost in the same damping levels compared to the damping level caused by the gains for the coupled rotor-body system. In case of $\zeta, \dot{\zeta}$-feedback regressing lead-lag motion is slightly better damped for the gains of the coupled rotor-body system. For additional flap state feedback the isolated blade gains even result in higher regressing lead-lag damping. But due to the lower gains of the flap states, the impact of the $\zeta, \dot{\zeta}$-feedback on other eigen modes, especially the pitch mode Θ/β_C, is not avoided. Actually, in the present case this impact on the pich mode is very low and probably tolerable.

Finally, Fig.16 presents closed loop damping for the lead-lag motion of the isolated blade and regressing lead-lag damping versus advance ratio at 92% Ω_{nom}. The gains are optimized for three advance ratios, i.e. hover case, $\mu = 0.2$ and $\mu = 0.4$, for both, isolated blade and coupled rotor-body system. To get continously gain scheduling, the gains are approximated by a quadratic function, using these three optimization points. The curves for G_ζ of both systems as well as the curve for $G_{\dot{\zeta}}$ of the isolated blade are parabolic, but the curve for $G_{\dot{\zeta}}$ of the coupled rotor-body system is more or less linear. The gains of the isolated blade varies more with forward speed. The lead-lag motion of the isolated blade is now better damped than applying gains optimized for hover, only. Still there exists a strong decrease of damping to a local minimum at $\mu = 0.33$. This is different for the coupled rotor-body system. Applying the gains optimized for the coupled rotor body system, regressing lead-lag damping slightly increases in the whole flight regime. A small local minimum is found at $\mu = 0.1$. However, applying the isolated blade gains to the coupled rotor-body system leads to a more intense rise in regressing lead-lag damping. Thus, regressing lead-lag motion is even better damped than the lead-lag motion of the isolated blade for advance ratios between $\mu = 0.28$ and $\mu = 0.45$. This is due to the high value of G_ζ and the low value of $G_{\dot{\zeta}}$, intensifying the former low coupling of regressing lead-lag and body pitch mode Θ/β_C, which results in a shift of damping between these two modes. Consequently, body pitch mode is destabilized and the eigen frequency is increased. Detailed investigations have to be done to evaluate the impact on handling qualities. Of course, the controller optimized for the coupled rotor-body system will also influence body-pitch mode, but this effect is kept low through gain limitation. Additional feedback of flap states could solve the problem of affecting body dynamics and body damping levels.

These explanations demonstrate the simplicity of the IBC approach to provide considerable regressing lead-lag damping throughout the whole flight regime with lag rate and deflection feedback, only. An optimization of gains for an isolated blade is possible and leads to good results. But special attention has to be paid to the influence of feedback loops on handling qualities.

4 Outlook and Conclusion

This study examinate active control of hingeless rotor helicopter. It has been shown that active control either through a conventional swashplate within SAS or through rotating actuators for IBC is a viable means to increase rotor-body damping levels for the helicopter on ground and in airborne state. Stability results have been presented for the open loop case and for the closed loop system using multi-variable feedback control. Four different controllers have been studied. Two SAS-controllers, the first feeding back roll and pitch rate and the second roll and pitch rate and cyclic lead-lag states as well as two IBC-controllers, one using only lead-lag states and the second lead-lag and flap states. The four controllers are compared to each other. Regarding the IBC approach additional controller designs and stability results have been performed for the isolated blade.
From these results, the following conclusions can be drawn :

- Roll and pitch feedback can suppress ground resonance, but additional feedback of cyclic lead-lag states is more effective and provides sufficient stability margins. Furthermore, the influence of the controllers on other eigen modes for the helicopter on ground is negligible.
- The results for the IBC-controllers to suppress ground resonance are less promising. Lead-lag states feedback mainly leads to a frequency shift of coalescence point. Due to the strong coupling of body and flap modes, flap states feedback can influence rotor-body interaction and thus increases regressing lead-lag damping.
- The controller design for both systems at one coalescence point is not able to prevent system instabilities at other rotor rotational speeds.
- Neglecting body states will not succeed in designing appropriate IBC-controllers for ground resonance suppression.
- The SAS approach seems to be preferable for suppression of ground resonance.
- Roll and pitch feedback can improve regressing lead-lag damping for the helicopter in airborne condition, but results are very poor. Additional cyclic lead-lag states feedback results in moderate damping margins in the whole flight regime. The SAS approach highly affects handling qualities and the implementation of filters seems to be unavoidable.
- Using the IBC approach, enormous damping levels for the lead-lag motion of the isolated blade as well as for the regressing lead-lag motion can be reached. Even with a simple $\zeta, \dot{\zeta}$-contoller results are very promising.
- The effect of IBC-controllers on handling qualities are low, but additional flap states feedback not only increases damping but also weakens adverse effects on system dynamics.
- For the present configuration both IBC-controllers stabilizes regressing lead-lag damping in the analyzed range of rotor speeds without gain scheduling. Because of lower damping ratios this might be not possible for SAS-controllers.
- Simple IBC-controller design for the whole range of advance ratio is possible without scheduling of gains. An optimization of feedback gains for the helicopter in hover will be most suitable.
- Controller design for the isolated blade is a good estimate to IBC-controllers for the coupled rotor-body system. But adverse effects on handling qualities have to be evaluated.
- The IBC approach seems to be preferable for augmenting regressing lead-lag damping for the helicopter in airborne condition.

More general conclusions are :

- The IBC concept is feasible if the coupling of body and rotor modes is low and the rotor system is mainly determined by isolated blade characteristics. Concerning the present configuration this situation occurs for the helicopter in the airborne state for a wide range of rotor speeds.
- If the coupling of body and rotor modes is high, the results for the IBC system are rather poor. In this case the SAS approach is very effective, since the control through the swashplate mainly affects rotor-flap and body modes. This situation arises for regressing lead-lag and body interaction in ground resonance.

Due to these promising results, further investigations concerning the potential of IBC to augment system stability are justified and necessary for developing an active control concept for future rotorcrafts. Some interesting aspects include :

- Consider more sophisticated models with elastic blade deflection and other important modelling effects.
- Implementing actuator and sensor dynamics to the feedback loops for realsitic controller design.
- Analyzing the impact of the feedback loops on handling qualities in detail, using appropriate criterions (ADS 33, FAR 27 & 29).
- Evaluate adverse effects on other stability or response problems, like vibration.

- Working on a concept for improving stability on ground and in air. Since rotating actuators are able to simulate a swashplate, a combination of the advantages of SAS and IBC seems to be possible.
- A combination of both systems would help to overcome stability problems of low frequency body modes in air. The SAS-system could contribute to improvements of handling qualities whereas the IBC-system is taking care of augmenting lead-lag damping.
- Analyzing the efficiency of "smart" trailing edge flap actuation to control lead-lag motion.

References

[1] G. Reichert, H. Huber. Influence of elastic coupling effects on the handling qualities of a hingeless rotor helicopter. *AGARD CP - 121*, pages 8.1 – 8.15, February 1973.

[2] R.A. Ormiston. Investigation of hingeless rotor stability. *Vertica*, 7(2):143 – 181, 1983.

[3] V. Klöppel, K. Kampa, B. Isselhorst. Aeromechanical aspects in the design of hingeless/bearingless rotor systems. *9th European Rotorcraft Forum*, Stresa, Italy, pages 57.1 – 57.25, September 13 – 15 1983.

[4] R.E. Donham, S.V. Cardinale, I.B. Sachs. Ground and air resonance characteristics of a soft in-plane rigid-rotor system. *Journal of the American Helicopter Society*, 14(4):33 – 41, October 1969.

[5] R.A. Ormiston. Aeromechanical stability of soft inplane hingeless rotor helicopters. *3rd European Rotorcraft Forum*, Aix-En-Provence, *France*, pages 25.1 – 25.22, September 7 – 9 1977.

[6] R.T. Lytwyn, W. Miao, W. Woitsch. Airborne and ground resonance of hingeless rotors. *Journal of the American Helicopter Society*, 16(2):2 – 9, April 1971.

[7] B. Panda, I. Chopra. Flap-lag-torsion stability in forward flight. *Journal of the American Helicopter Society*, 30(4):30 – 39, October 1985.

[8] D.H. Hodges, R.A. Ormiston. Stability of elastic bending and torsion of uniform cantilever rotor blades in hover with variable structural coupling. *NASA TN D-8192*, April 1976.

[9]
R.A. Ormiston, W.G. Warmbrodt, D.H. Hodges, D.A. Peters. Rotorcraft aeroelastic stability. *NASA CP-2495*, pages 353–529, 1988.

[10] R.A. Ormiston. The challenge of the damperless rotor. *22rd European Rotorcraft Forum*, Brighton, UK, pages 68.1 – 68.14, September 17 – 19 1996.

[11] H. Huber. Effect of torsion-flap-lag coupling on hingeless rotor stability. *29th Annual National Forum of the American Helicopter Society*, pages 1–14, May 1973.

[12] R.A. Ormiston, D.H. Hodges. Linear flap-lag dynamics of hingeless helicopter rotor blades in hover. *Journal of the American Helicopter Society* , 17(2):2 – 14, April 1972.

[13] R.G. Loewy, M. Zotto. Influence of pitch-lag coupling on damping requirements to stabilize ground/air resonance. *Journal of the American Helicopter Society*, 37(4):68–71, October 1992.

[14] P. Roesch, M. Allongue, M. Achache. Towards generalized active control of helicopters. *19th European Rotorcraft Forum*, Cernobbio (Como), Italy, pages A1.1 – A1.19, September 14 – 16 1990.

[15] M.I. Young, D.J. Bailey, M.S. Hirschbein. Open and closed loop stability of hingeless rotor helicopter air and ground resonance. *AHS/NASA-Ames Specialists' Meeting on Rotorcraft Dynamics*, pages 1 – 32, February 13 – 15 1974.

[16] F.K. Straub, W. Warmbrodt. The use of active controls to augment rotor/fuselage stability. *Journal of the American Helicopter Society* , 30(3):13 – 22, July 1985.

[17] F.K. Straub. Optimal control of helicopter aeromechanical stability. *11th European Rotorcraft Forum*, London, England, pages 77.1 – 77.16, September 10 – 13 1985.

[18] M.D. Takahashi, P.P. Friedmann. Design of a simple active controller to suppress helicopter air resonance. *44th Annual Forum of the American Helicopter Society*, pages 305 – 315, June 1988.

[19] M.D. Takahashi, P.P. Friedmann. A model for active control of helicopter air resonance in hover and forward flight. *14th European Rotorcraft Forum*, Milano, Italy, pages 57.1 – 57.23, September 20 – 23 1988.

[20] Ch. Kessler, G. Reichert. Active control of ground and air resonance including transition from ground to air. *20th European Rotorcraft Forum*, Amsterdam, Netherlands, pages 64.1 – 64.17, October 4 – 7 1994.

[21] R. Kube. New aspects of Higher Harmonic Control on a four-bladed hingeless helicopter. *Journal of the American Helicopter Society*, 37(3):61 – 68, July 1992.

[22] R. Kube, B.v.d. Wall, K.-J. Schultz. Mechanisms of vibration and BVI noise reduction by Higher Harmonic Control. *20th European Rotorcraft Forum, Amsterdam, Netherlands*, pages 27.1 – 27.23, October 4 – 7 1994.

[23] P. Richter, T. Schreiber. Theoretical Investigations and wind-tunnel tests with HHC-IBC. *20th European Rotorcraft Forum,* Amsterdam, Netherlands, pages 71.1 – 71.15, October 4 – 7 1994.

[24] N.D. Ham. Helicopter Individual Blade Control and its applications. *9th European Rotorcraft Forum,* Stresa, Italy, pages 56.1 – 56.11, September 13-15 1983.

[25] N.D. Ham. A simple system for helicopter Individual Blade Control using modal decomposition. *Vertica,* 4(1):23 – 28, 1980.

[26] N.D. Ham. Helicopter Individual Blade Control research at MIT 1977-1985. *Vertica,* 11(1/2):109 – 122, 1987.

[27] N.D. Ham, T.R. Quackenbush. A simple system for helicopter individual-blade-control and its application to stall flutter suppression. *7th European Rotorcraft Forum,* Garmisch-Partenkirchen, Germany, pages 76.1 – 76.28, September 8 – 11 1981.

[28] N.D. Ham. Helicopter gust alleviation, attitude stabilisation, and vibration alleviation using individual-blade-control through a conventional swashplate. *11th European Rotorcraft Forum,* London, England, pages 75.1 – 75.5, September 10 – 13 1985.

[29] N.D. Ham, B.L. Behal, R.M. McKillip. Helicopter rotor lag damping augmentation through individual-blade-control. *Vertica,* 7(4):361 – 371, 1983.

[30] N.D. Ham. Helicopter individual-blade-control: Promising technology for the future helicopter. *21th European Rotorcraft Forum,* St. Petersburg, Russia, pages 9.1 – 9.6, August 30 – September 1 1995.

[31] N.D. Ham, R.M. McKillip JR. Research on measurement and control of helicopter rotor response using blade-mounted accelerometers. *7th European Rotorcraft Forum,* Berlin, Germany, pages 91–77.1 – 91–77.7A, September 24-26 1991.

[32] D.Teves, V. Klöppel, P. Richter. Development of active control technology in the rotating system, flight testing and theoretical investigation. *19th European Rotorcraft Forum,*Avignon, France, pages 89.1 – 89.13, September 15 – 18 1992.

[33] P. Richter, A. Blaas. Full scale wind tunnel investigation of an individual blade control system for Bo 105 hingeless rotor. *19th European Rotorcraft Forum,* Cernobbio (Como), Italy, pages G5.1 – G5.12, September 14 – 16 1990.

[34] G. Reichert, U. Arnold. Active control of helicopter ground and air resonance. *16th European Rotorcraft Forum,* Glasgow, Scotland, pages III.6.2.1 – III.6.2.14, September 18 – 20 1990.

[35] Ch. Kessler, G. Reichert. Active control to augment rotor lead-lag damping. *22nd European Rotorcraft Forum,* Brighton, UK, pages 10.1 – 10.16, September 17 – 19 1996.

[36] P.P. Friedmann. Helicopter rotor dynamics and aeroelasticity: Some key ideas and insights. *Vertica,* 14(1):101–121, 1990.

[37] D.A. Peters. The importance of steady and dynamic inflow on the stability of rotor-body systems. *NASA Conference Publication 10007, 'Integrated Technology Rotor Methodology Assessment Workshop',* pages 181 – 201, June 1983.

[38] P.P. Friedmann, C. Venkatesan. Influence of unsteady aerodynamic models on aeromechanical stability in ground resonance. *Journal of the American Helicopter Society,* 31(1):65 – 74, 1986.

[39] D.M. Pitt, D.A. Peters. Theoretical prediction of dynamic-inflow derivatives. *6th European Rotorcraft Forum,* Bristol, England, pages 47.1 – 47.18, September 16 – 19 1980.

[40] K.H. Hohenemser, S. Yin. Some applications of the method of multiblade coordinates. *Journal of the American Helicopter Society,* 17(3):3 – 12, July 1972.

[41] W. Johnson. *Helicopter Theory.* Princeton University Press, 1980.

[42] I. Chopra. Perspectives in aeromechanical stability of helicopter rotors. *Vertica,* 14(4):457 – 508, 1990.

[43] W. Johnson. Influence of unsteady aerodynamics on hingeless rotor ground resonance. *Journal of Aircraft,* 19(8):668 – 673, 1982.

[44] J. Jang, I. Chopra. Ground and air resonance of an advanced bearingless rotor in hover. *Journal of the American Helicopter Society,* 33(3):20 – 29, July 1988.

[45] J.M. Wang, J. Jang, I. Chopra. Air resonance stability of hingeless rotors in forward flight. *Vertica,* 14(2):123 – 136, 1990.

[46] H.C. Curtiss Jr. Stability and control modelling. *Vertica,* 12(4):381 – 394, 1988.

[47] J. Ewald. *Untersuchung zur aeromechanischen Stabilität des Hubschraubers.* Dissertation, ZLR-Forschungsbericht 91-05, Zentrum f"ur Luft- und Raumfahrttechnik der Technischen Universität Braunschweig, Braunschweig, 1991.

[48] F. K. Straub. A feasibility study of using smart materials for rotor control. *49th Anual Forum of the American Helicopter Society,* St. Louis, Missouri, pages 1321 – 1333, May 19 – 21 1993.

[49] H. Strehlow, H. Rapp. Smart materials for helicopter rotor active control. *AGARD/SMP Spec. Mtg. on Smart Strucutres for Aircraft and Spacecraft,* Lindau, Germany, pages 5.1 – 5.16, Oct. 1992.

[50] I. Chopra. Development of a smart rotor. *19th European Rotorcraft Forum* Cernobbio,Italy, pages 6.1 – 6.18, Sep. 14 – 16 1993.

[51] W.S. Levine, M. Athenas. On the determination of the optimal constant output feedback gains for linear multivariable systems. *IEEE Transactions on Automatic Control,* 15(1):44 – 48, February 1970.

[52] O. Föllinger. Entwurf konstanter Ausgangsrückführungen im Zustandsraum. *Automatisierungstechnik,* 34(1):5 – 15, Januar 1986.

[53] M.E. Wasikowski. *Optimal Output Vector Feedback, Theory Manual.* Georgia Tech Research Institute, Atlanta, Georgia, 1992.

[54] T. Krysinski. Active control of aeromechanical stability. *AGARD-CP-592,* pages 32.1 – 32.25, April 1997.

Concept	SAS						IBC			
controller	p	q	ζ_C	ζ_S	$\dot{\zeta}_C$	$\dot{\zeta}_S$	ζ	$\dot{\zeta}$	β	$\dot{\beta}$
1	0.234 193.6°	6.649 21.7°	-	-	-	-	-0.8	-1.8	-	-
2	0.372 34.4°	2.618 32.1°	0.156 279.2°	0.764 209.9°	0.728 212.9°	0.049 247.1°	-0.8	-1.8	0.8	1.0

Table 2: Optimized Feedback Gains and Phases for the Helicopter on Ground

Concept	SAS						IBC			
controller	p	q	ζ_C	ζ_S	$\dot{\zeta}_C$	$\dot{\zeta}_S$	ζ	$\dot{\zeta}$	β	$\dot{\beta}$
1	10.063 324.7°	8.015 100.1°	-	-	-	-	1.0	-0.7	-	-
2	14.899 194.3°	11.067 84.4°	0.577 189.6°	0.456 150.7°	2.149 192.3°	1.484 340.2°	1.5	-0.9	0.5	0.7

Table 3: Optimized Feedback Gains and Phases for the Helicopter in Hover

System	Isolated Blade				Rotor-Body			
controller	ζ	$\dot{\zeta}$	β	$\dot{\beta}$	ζ	$\dot{\zeta}$	β	$\dot{\beta}$
1	1.023	-0.905	-	-	1.0	-0.7	-	-
2	1.582	-1.643	0.483	0.412	1.5	-0.9	0.5	0.7

Table 4: IBC-Gains Optimized for the Isolated Blade and the Coupled Rotor-Body System in Hover

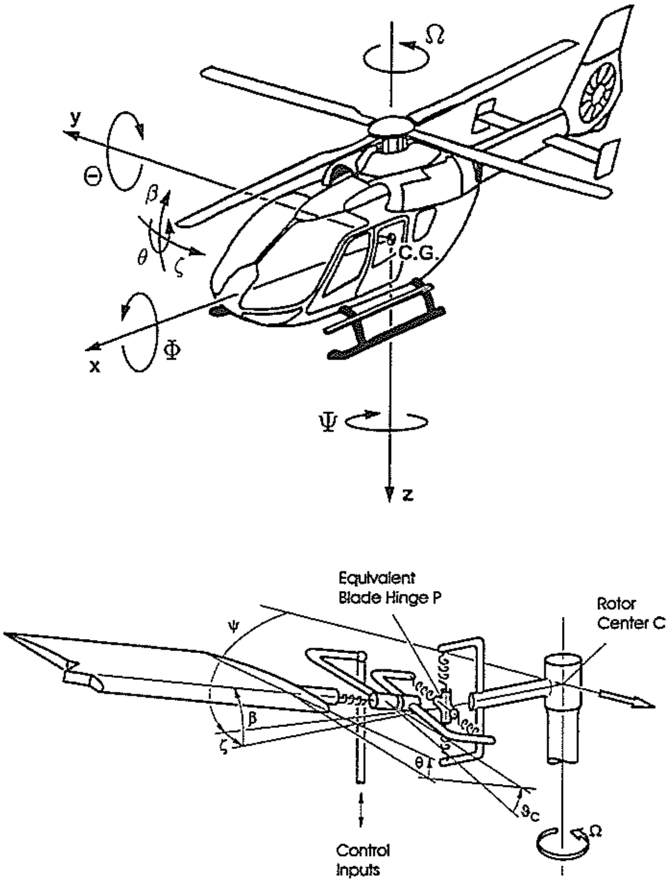

Figure 1: Mathematical Helicopter Model

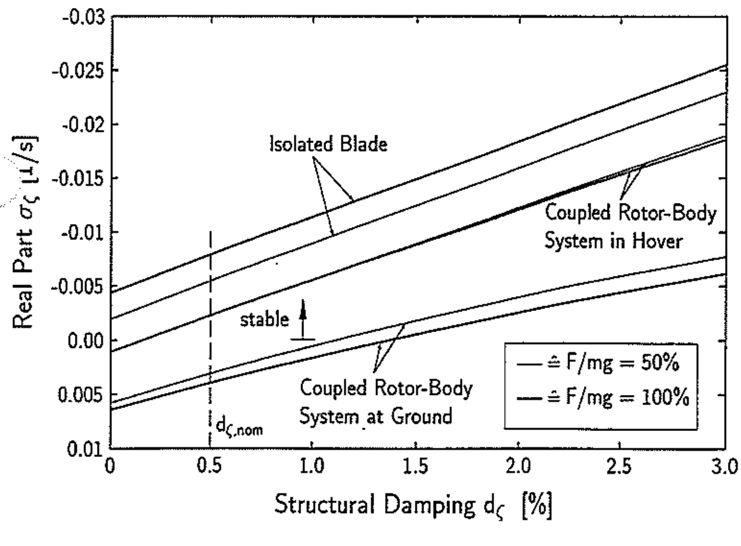

Figure 2: Damping vs. Lead-Lag Structural Damping for the Lead-Lag Motion of the Isolated Blade and Regressing Lead-Lag, $\Omega = 93\%\ \Omega_{nom}$

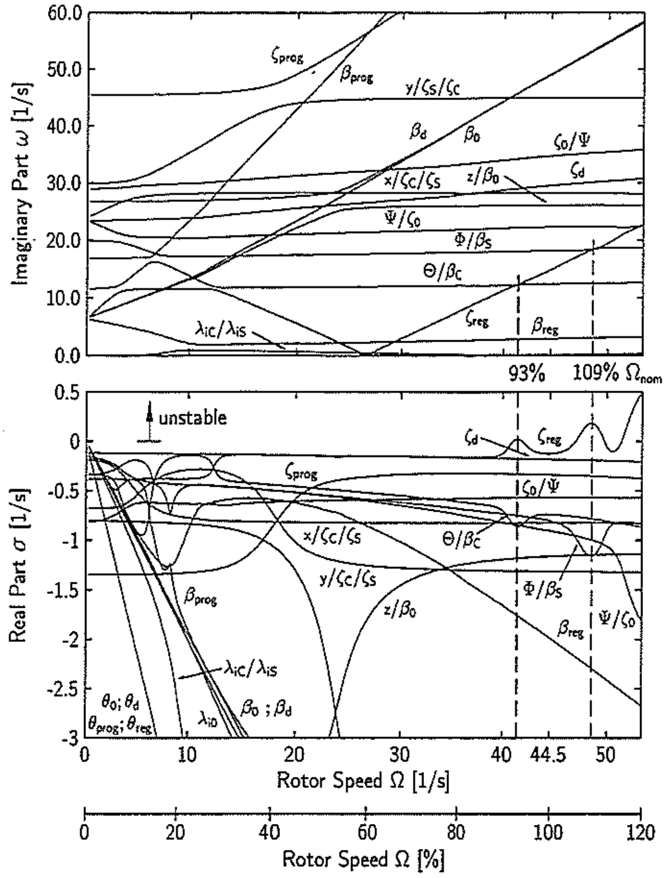

Figure 3: Eigen Values of the Coupled Rotor-Body System on Ground, F/mg = 0%

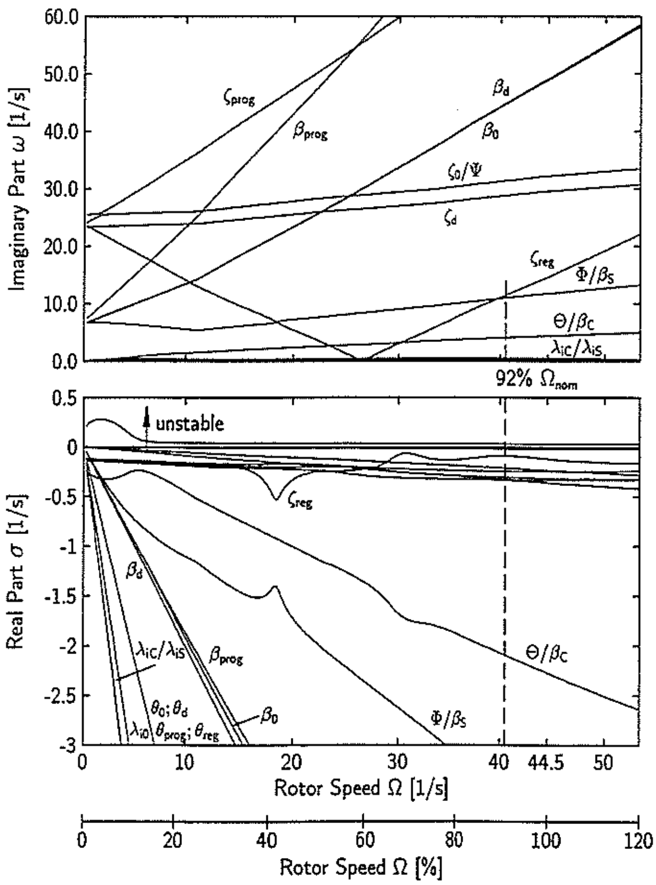

Figure 4: Eigen Values of the Coupled Rotor-Body System in Hover, $\vartheta_0 = 12°$

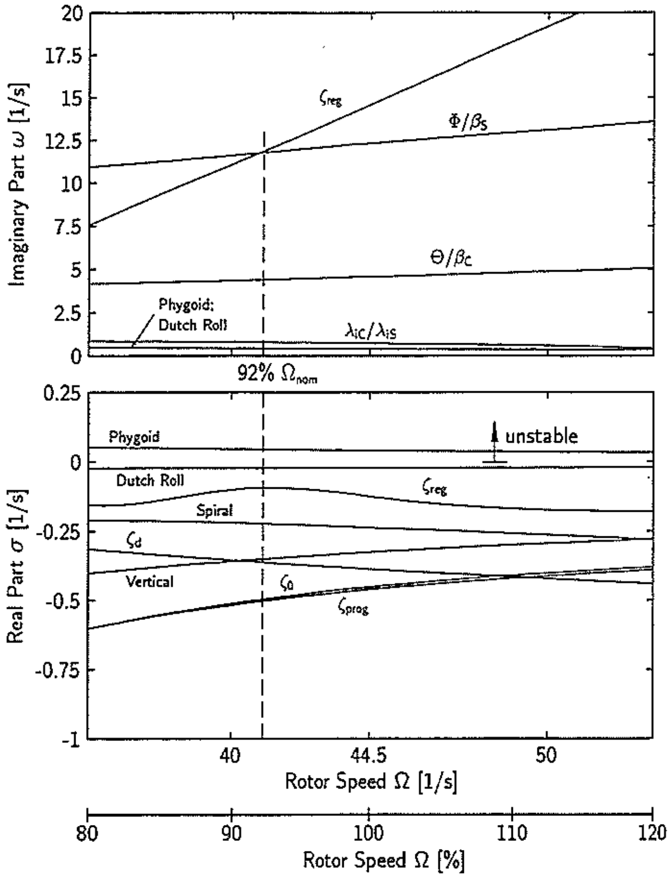

Figure 5: Eigen Values of the Coupled Rotor-Body System in Hover, Propulsive Trim

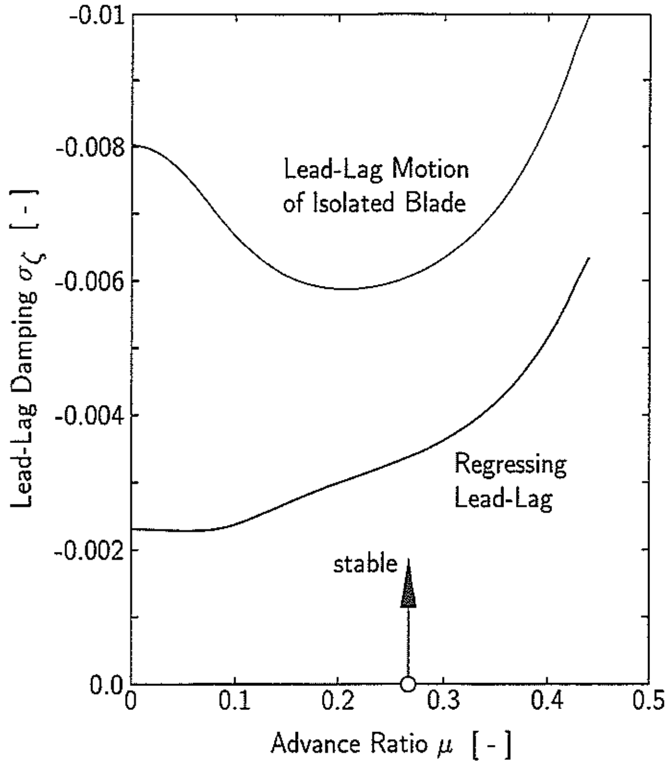

Figure 6: Damping vs. Advance Ratio for Isolated Lead-Lag Motion and Regressing Lead-Lag, $\Omega = 92\%\ \Omega_{nom}$

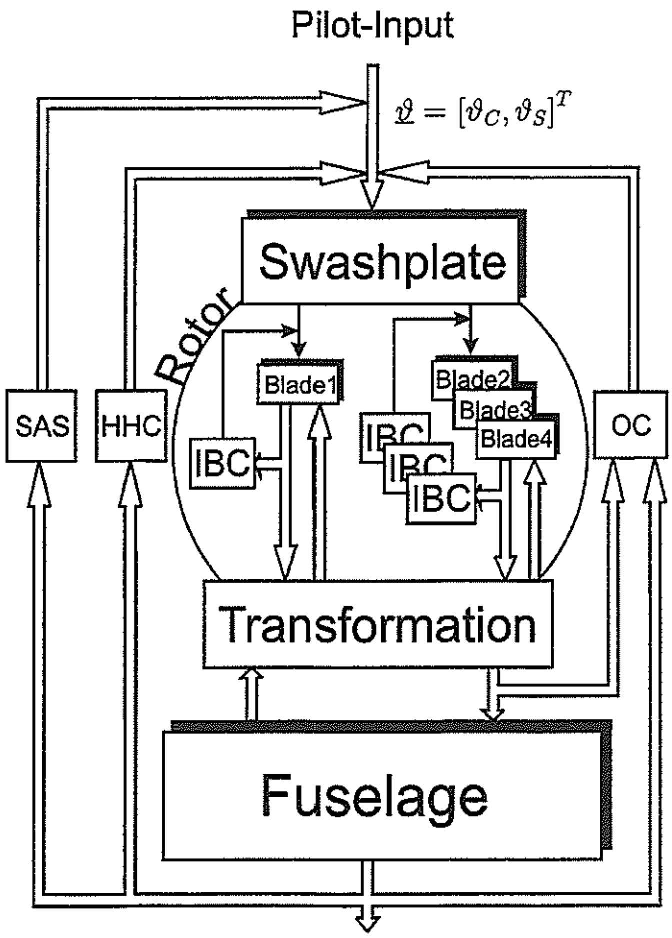

Figure 7: Active Control Concepts for Rotor-Body Stability Problems

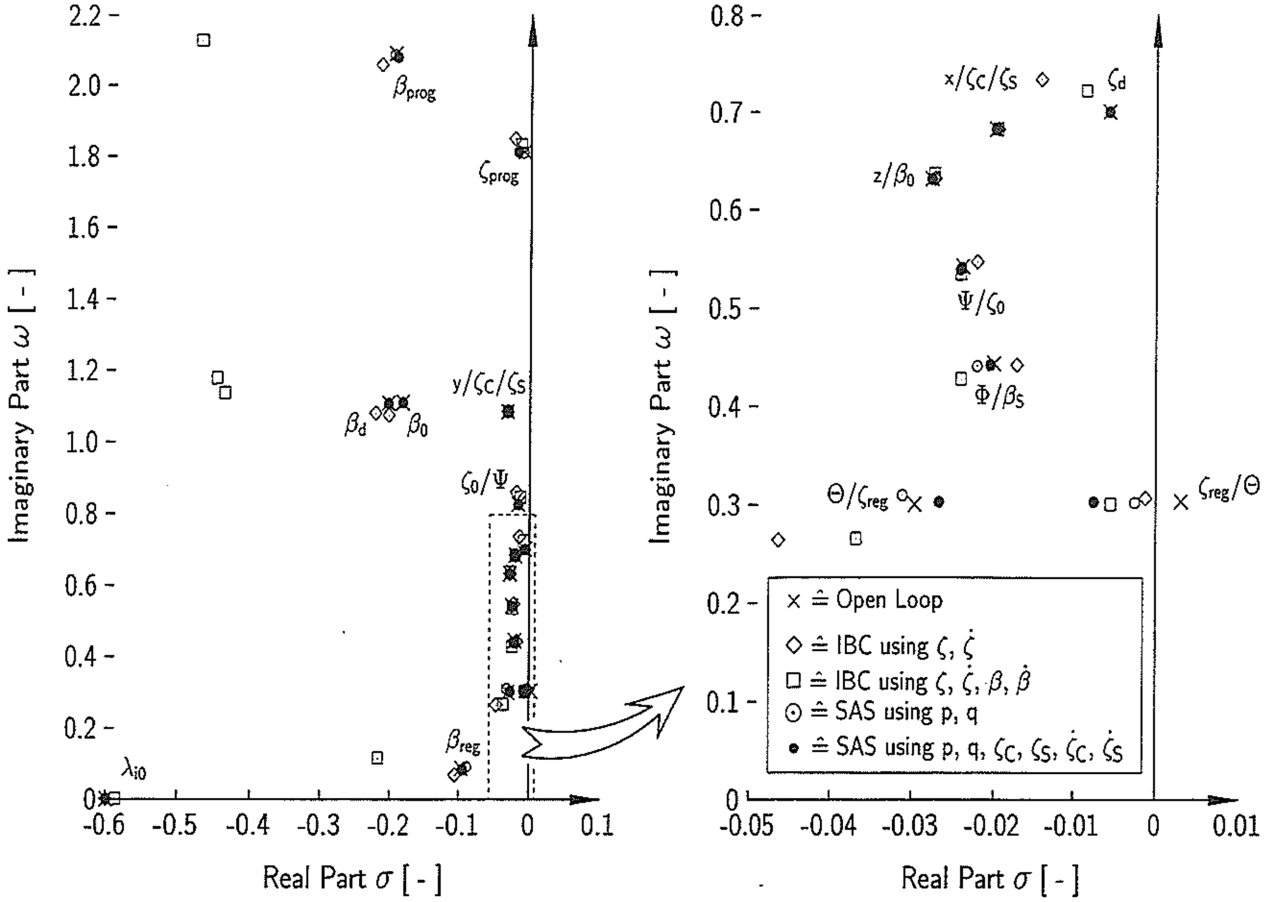

Figure 8: Open and Closed Loop Poles for Different Controllers, Helicopter on Ground, $\Omega = 93\%\ \Omega_{nom}$, F/mg = 50%

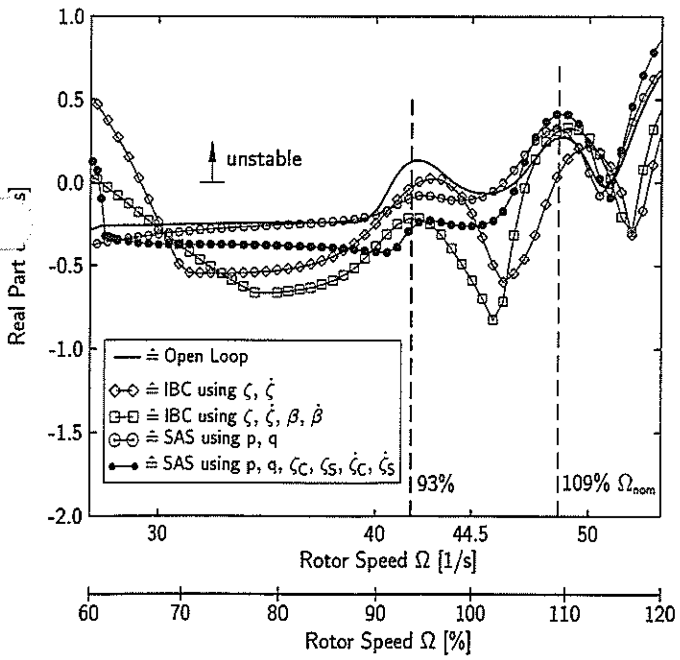

Figure 9: Open and Closed Loop Damping versus Rotor Speed for Regressing Lead-Lag or Coupling Body Modes, Helicopter on Ground, F/mg = 50%

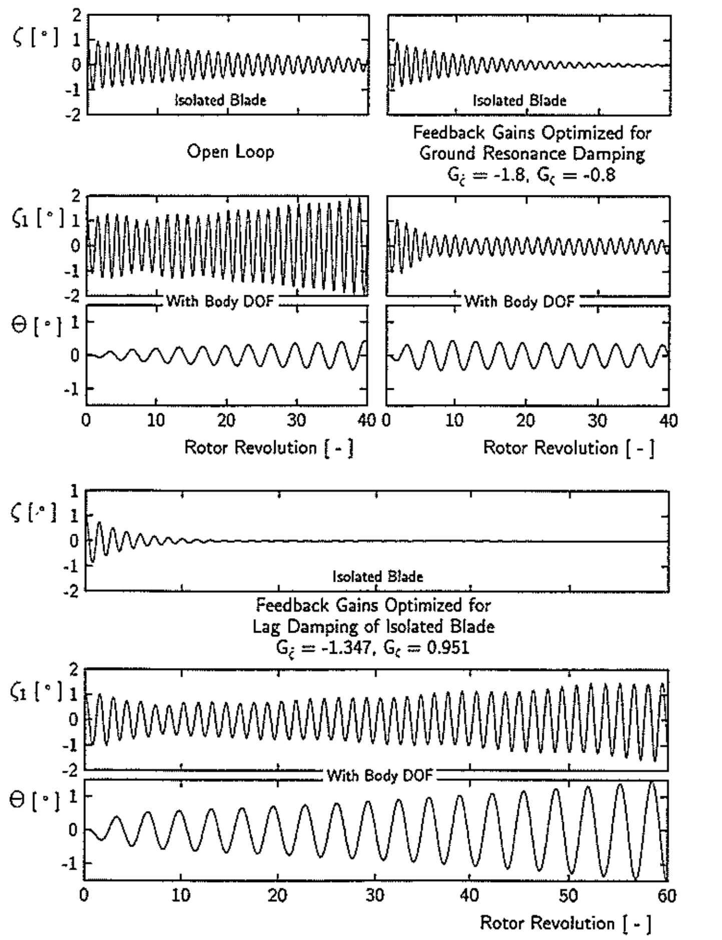

Figure 10: Lead-Lag Damping Augmentation through IBC, Isolated Blade Compared with Helicopter on Ground, $\Omega = 93\%\ \Omega_{nom}$, F/mg = 50%

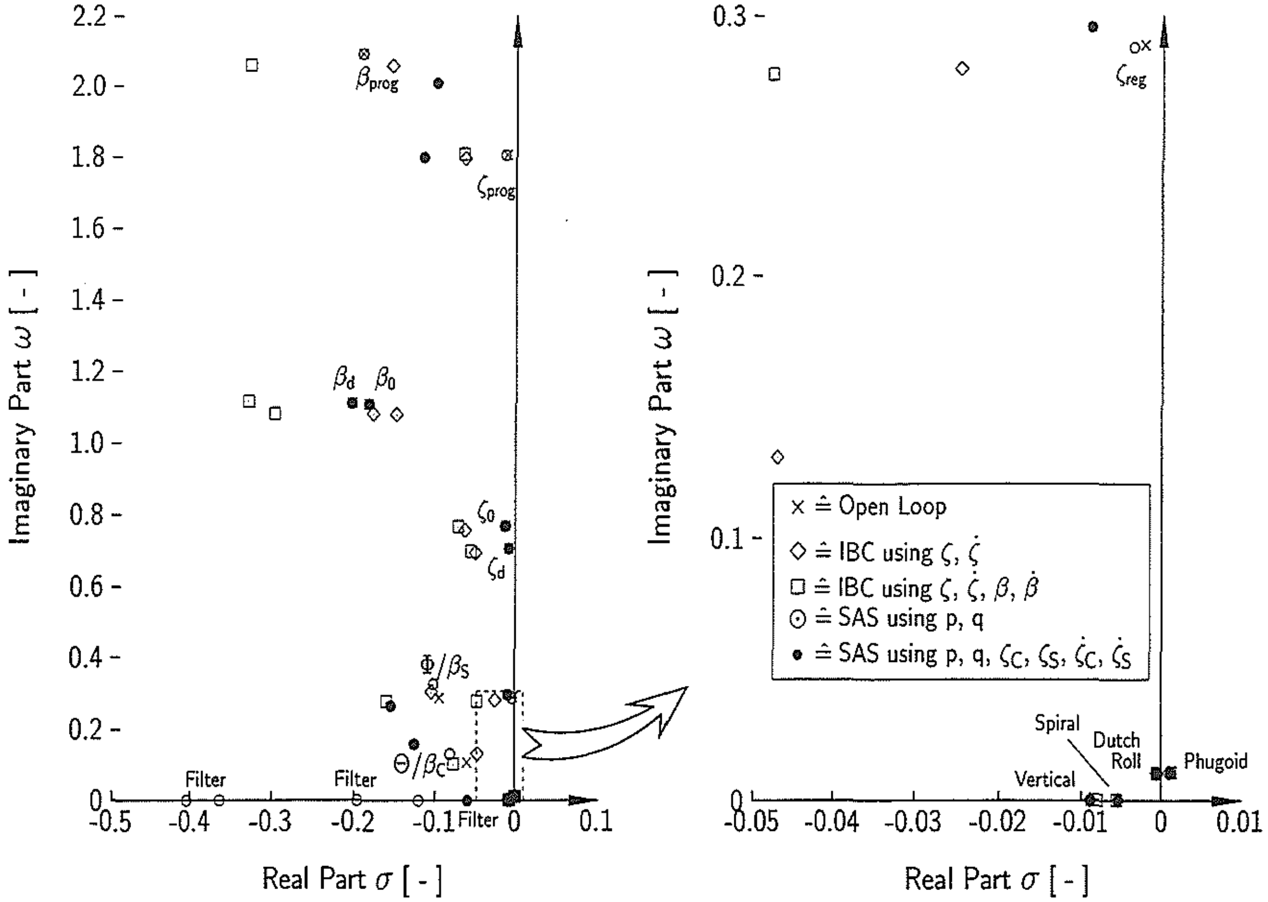

Figure 8: Open and Closed Loop Poles for Different Controllers, Hover Condition, $\Omega = 92\%\ \Omega_{nom}$

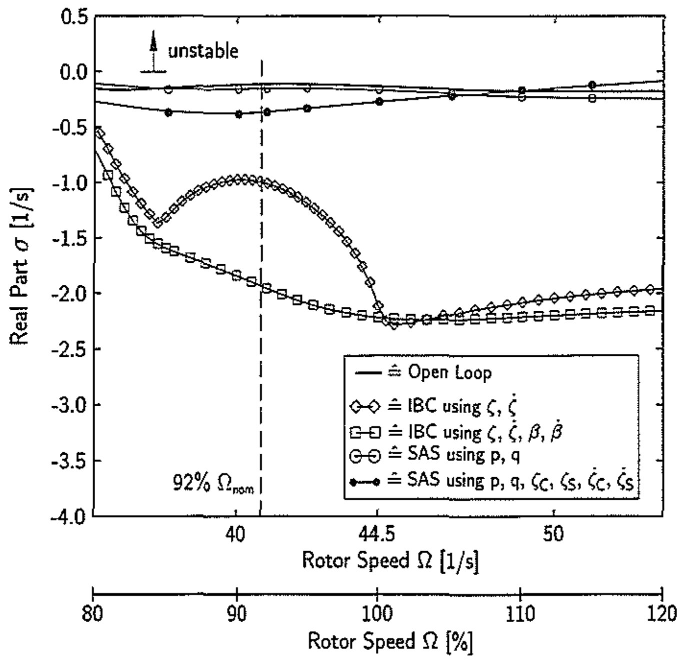

Figure 9: Open and Closed Loop Damping versus Rotor Speed for Regressing Lead-Lag or Coupling Body Modes, Helicopter in Hover

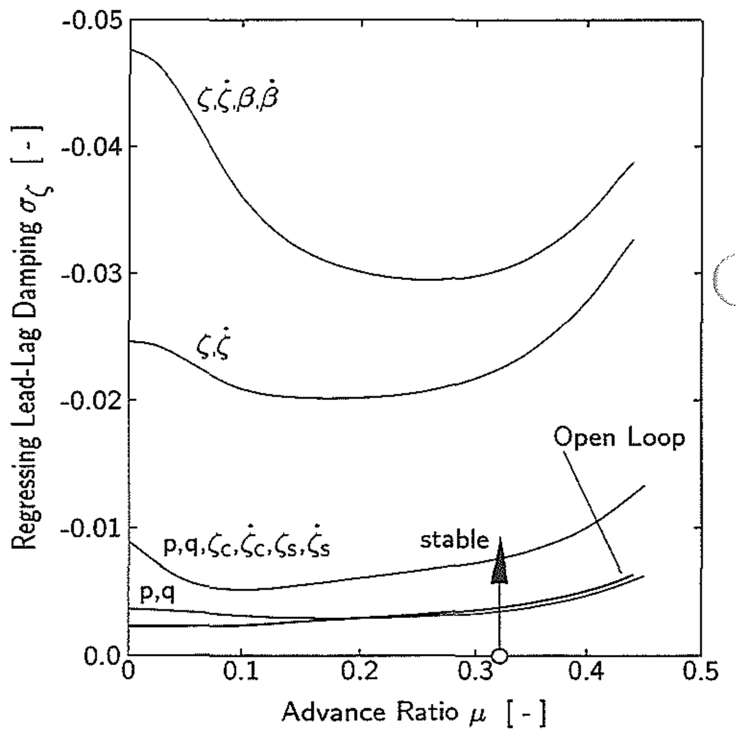

Figure 10: Regressing Lead-Lag Damping versus Advance Ratio for Open and Closed Loop System, Gains Optimized in Hover, $\Omega = 92\%\ \Omega_{nom}$

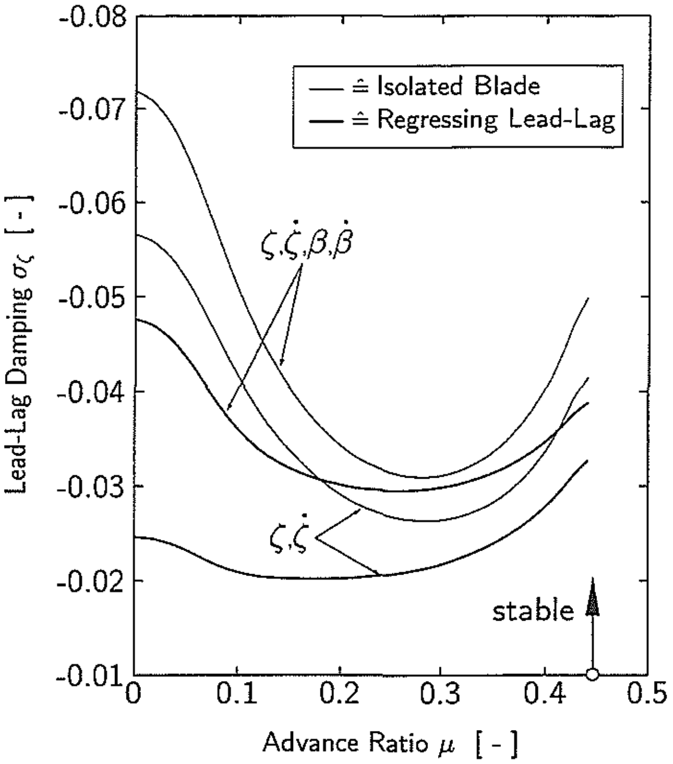

Figure 14: Closed Loop Damping vs. Advance Ratio for Lead-Lag Motion of Isolated Blade and Regressing Lead-Lag, Hover-Gains for IBC, $\Omega = 92\%\ \Omega_{nom}$

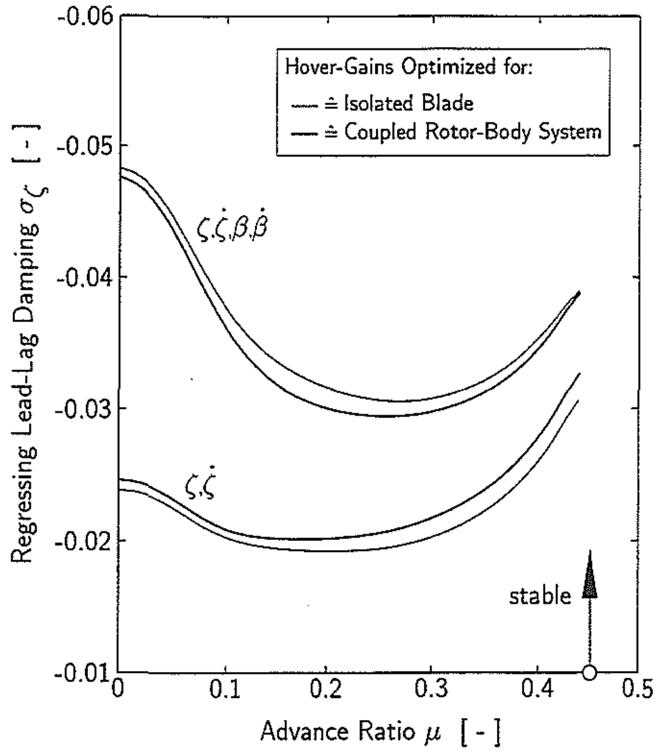

Figure 15: Closed Loop Regressing Lead-Lag Damping vs. Advance Ratio, Effect of Isolated Blade Gains on Coupled Rotor-Body System, $\Omega = 92\%\ \Omega_{nom}$

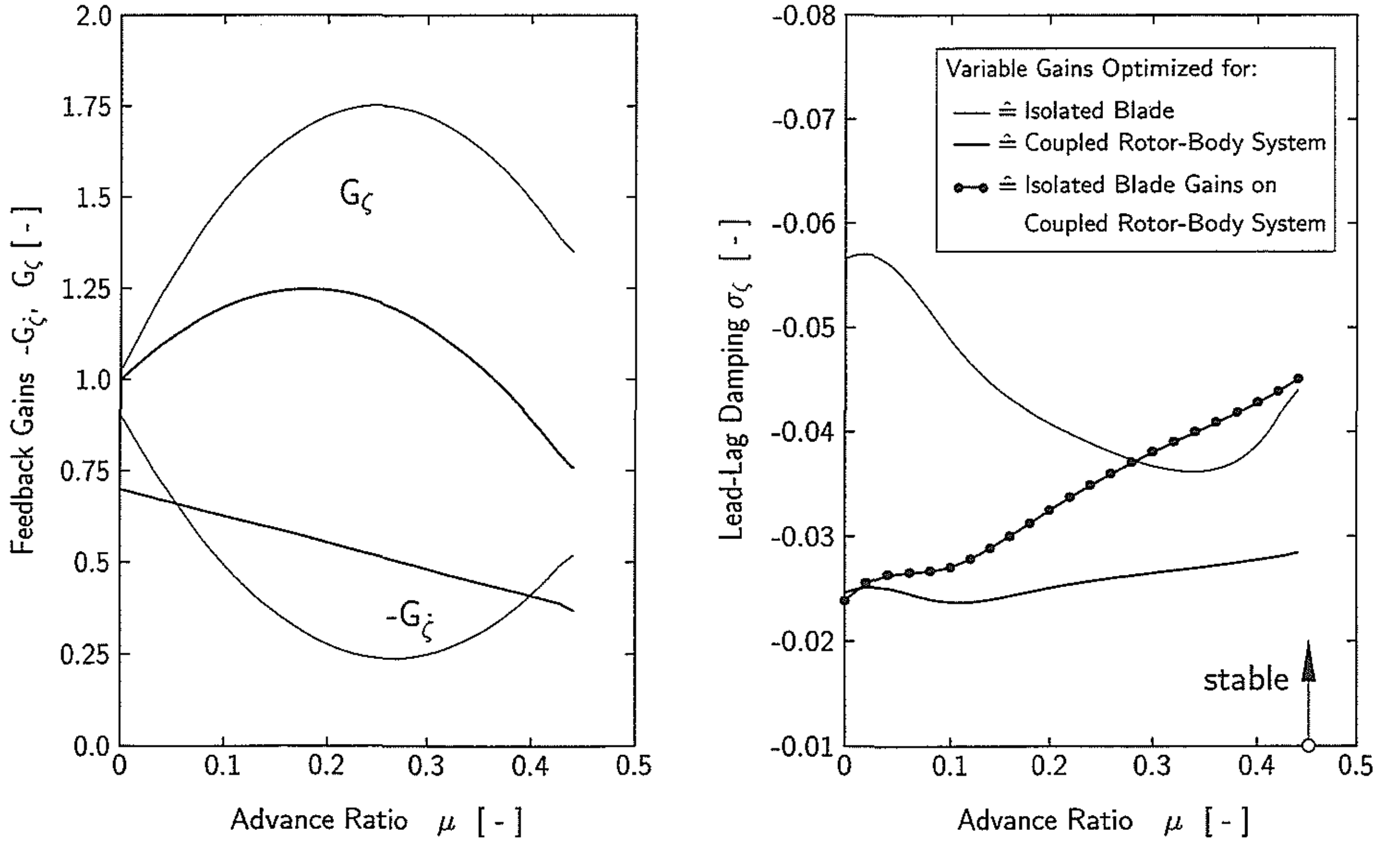

Figure 16: Feedback Gains and Losed Loop Damping vs. Advance Ratio for Isolated Lead-Lag Motion and Regressing Lead-Lag, $\zeta,\dot{\zeta}$-Feedback, $\Omega = 92\%\ \Omega_{nom}$